Automatic P-Phase Picking Based on Local-Maxima Distribution

Costas Panagiotakis, Eleni Kokinou, and Filippos Vallianatos

***Abstract*—In this paper, we propose a method for the automatic identification of P-phase arrival based on the distribution of local maxima (LM) in earthquake seismograms. The method efficiently combines energy and frequency characteristics of the LM distribution (LMD). The P detection is mainly based on the energy of a seismic event in the case the earthquake has higher amplitude than seismic background noise. Otherwise, it is based on the frequency of LM. Thus, the method provides robust detection of P-phase arrival in any quality type of seismic data. Moreover, it uses two sequential sliding signal windows yielding very high accuracy on the P-phase estimation. A hierarchical P-phase detection algorithm dramatically reduces the computational cost, making possible a real-time implementation. Experimental results from a large database of more than 80 low, medium, and high signal-to-noise ratio seismic events and comparison with existing methods in the literature indicate the reliable performance of the proposed scheme.**

***Index Terms*—Automatic picking, P-phase arrival identification, seismic-signal analysis, signal segmentation.**

I. Introduction

EARTHQUAKE is the shaking and vibration at the surface of the earth resulting from underground movement along a fault plane or from volcanic activity, producing seismic waves. Seismic waves are studied through records of mechanical vibrations of the earth (seismic traces). These records register the effect from different types of waves originating from a certain point or plane, i.e., the earthquake source in the interior of the Earth on its surface [1].

A seismic signal consists of several different phases, which characterize the type of the considered seismic signal. P and S phases are considered as the most important of them. P phases are longitudinal waves that propagate along the direction of seismic-wave propagation. S phases are transverse waves that propagate perpendicular to the direction of seismic-wave propagation [2]. Accurate picking of P and S phases constitutes the most important step for earthquake location, tomographic study, and for any further understanding of crustal and upper mantle structure [3]. Large data sets must be analyzed in order to reveal P arrival times and further construct the seismic tomography for the studied area. During the last decades, a lot of work has been done for developing algorithms able to automatically detect the earthquake P [4]–[8] and S [9], [10] wave arrival.

Most approaches address the P-phase picking problem by focusing either on energy variations or using high-order statistics (e.g., kurtosis or skewness [1]), yielding good results on specific earthquake events. In this paper, we have developed an automatic P-phase picker that combines robust energy and frequency characteristics, yielding high-accuracy results under any type of seismic data. We have introduced the local-maxima distribution (LMD), as a robust and well-understandable feature that suffices to discriminate the P phase. The main contribution of this paper is that we take into account the energy and frequency changes.

The rest of this paper is organized as follows. Section II describes the problem formulation and the proposed features. Section III presents the proposed scheme. Experimental results and comparisons are given in Section IV. Finally, the conclusions are provided in Section V.

II. Properties of LMD

A. LM Estimation

Let $\{Z(k)\}$ be the absolute value of z component of a given seismogram. The set of the LM belonging in a time window W is given by the following:

$$LM(W) = \{k \in W : Z(k) > \max\{Z(k-1), Z(k+1)\}\}. \tag{1}$$

We have used the absolute value in order to get, at the same time, the local minima of the seismogram when the given signal has zero mean, as well as its real local minima that correspond to LM of $\{Z(k)\}$. LMD has been successfully applied on human-motion analysis estimating the gait period [11]. It holds that when the given signal is a smooth one (e.g., a series of cosines), then it can be reconstructed with good accuracy by the interpolation of its LM (see Fig. 1). Moreover, the central period of the signal can be determined by the LM frequency. In addition, the part of the signal that corresponds to LM has locally very high energy. Therefore, it is less affected by noise, resulting to robust features. Consecutively, the LMD robustly encodes the properties of the given signal, providing data reduction, and keeping the low-frequency components of the signal. We have proposed two almost independent characteristics, the energy and the frequency of the LM set. In order to prove this

Manuscript received April 29, 2007; revised December 27, 2007. This work was supported in part by the Greek General Secretariat of Research and Technology under the frame of Crete Regional Project 2000–2006 (M1.2): "An integrated system of seismic hazard monitoring and management in the front of the Hellenic arc," CRETE PEP_7 (KP_7).

C. Panagiotakis is with the Department of Computer Science, University of Crete, 71409 Heraklion, Greece (e-mail: cpanag@csd.uoc.gr).

E. Kokinou and F. Vallianatos are with the Laboratory of Geophysics and Seismology, Department of Natural Resources and Environment, Technological Educational Institute of Crete, 73133 Heraklion, Greece (e-mail: ekokinou@chania.teicrete.gr; fvallian@chania.teicrete.gr).

Digital Object Identifier 10.1109/TGRS.2008.917272

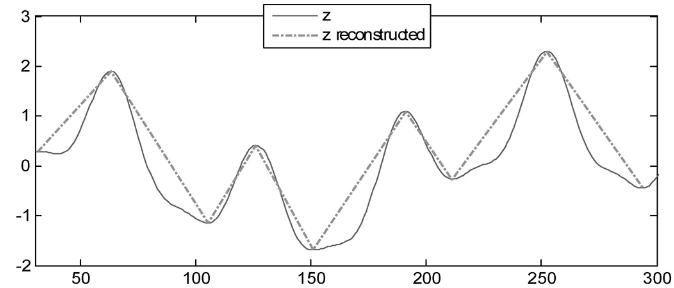

Fig. 1. Example of reconstruction by linear interpolation of LM set.

hypothesis, we have tested the Blomquist measure [12], defined as $V = (|n_1 - n_2|/n)$, where n is the number of data pairs, n_1 is the number of pairs with the same sign related to the median values of the two variables, and n_2 is the number of pairs with opposite signs. The empirical value obtained for V was about 0.07, showing an almost sure independence.

B. Energy of LM

The mean energy per sample of LM set $e(LM(W))$ is a robust and well-understandable feature.

$$e\left(LM(W)\right) = \frac{1}{|LM(W)|} \sum_{k \in LM(W)} Z^2(k). \tag{2}$$

$|LM(W)|$ denotes the number of LM set. It holds that a noise signal and an earthquake signal can participate to the components that correspond to the vicinity of zero-crossings part (low-energy part) and to the components that correspond to LM part (high-energy part). The energy histograms of an earthquake and a noise signal differ less than the LM-energy histograms (Fig. 2). In order to prove that, we used Earth movers distance (EMD) [13] applied on the histograms of Fig. 2. The EMD is based on the minimal cost that must be paid to transform one distribution into the other in a precise sense. It is more robust than histogram-matching techniques, since it can be applied on variable-length representations of the distributions that avoid quantization and other binning problems typical of histograms. However, due to its high-computational cost, EMD cannot be used on P-phase picking.

The EMD between energy histograms of the earthquake signal of Fig. 2(b), and the noise signal of Fig. 2(e) is $2.1 \cdot 10^{11}$, while the EMD between energy histograms of LM of the earthquake signal of Fig. 2(c) and the noise signal of Fig. 2(d) is $2.744 \cdot 10^{11}$. Therefore, the proposed feature can be used to discriminate real seismic events from noise signal, yielding slightly better results than the global signal energy, as our experiments have shown.

C. Frequency of LM

The frequency of LM set $f(LM(W))$ is defined by the ratio between the number of LM $|LM(W)|$ and the number of the corresponding signal samples $|W|$.

$$f\left(LM(W)\right) = \frac{|LM(W)|}{|W|}. \tag{3}$$

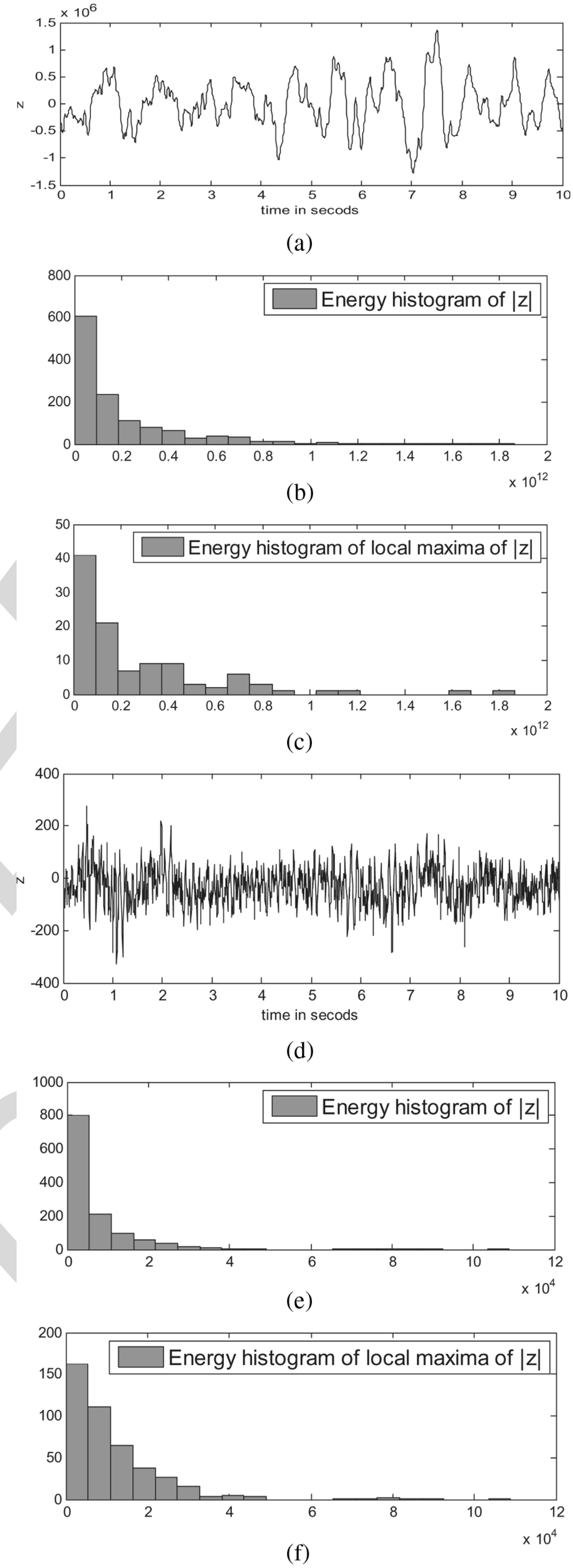

Fig. 2. Seismograms of (a) earthquake and (d) noise recordings. Histograms of $|z|^2$ component of (b) earthquake and (e) noise. Histograms of $|z|^2$ component of the LM set of (c) earthquake and (f) noise.

In the case of a noisy signal, the frequency of the LM set is getting a very high value. It holds that

$$0 < f\left(LM(W)\right) \leq 1/2. \tag{4}$$

For the case of uncorrelated noise (e.g., Gaussian white noise), it holds that $f(LM(W)) = 1/3$. This was proven experimentally using noise signals of considerable length, but it can also be proven theoretically as follows. Let as consider a random sequence $X(\cdot)$ of values. We select a specific sample $X(k)$. If $X(k)$ is a local maximum, then it should be greater than $X(k-1)$ and $X(k+1)$. However, $X(k-1)$, $X(k)$, and $X(k+1)$ are random and uncorrelated values, so the probability of $X(k)$ (one of three) to be a local maximum is 1/3. This probability is equal to the requested frequency. The frequency of LM set in a nonnoise signal is lower, and it corresponds to the central period of the signal (Fig. 1). Therefore, the frequency of the LM set can be used for signal/noise discrimination. Moreover, if the statistics of the signal vary, then the frequency will change with high probability. Fig. 3(b) and (d) shows the frequency of the LM set for the vertical component z [Fig. 3(a) and (c)] of January 8, 2006 earthquake (11:35:09.895 UTC, mb = 6.7, CMT Harvard routine analysis) and an aftershock (21:58 UTC, mb = 3.3, CMT Harvard routine analysis), occurred in northwestern area of Crete Island, Greece. It holds that the frequency of LM for the part of the signal corresponding to the real seismic event is minimized.

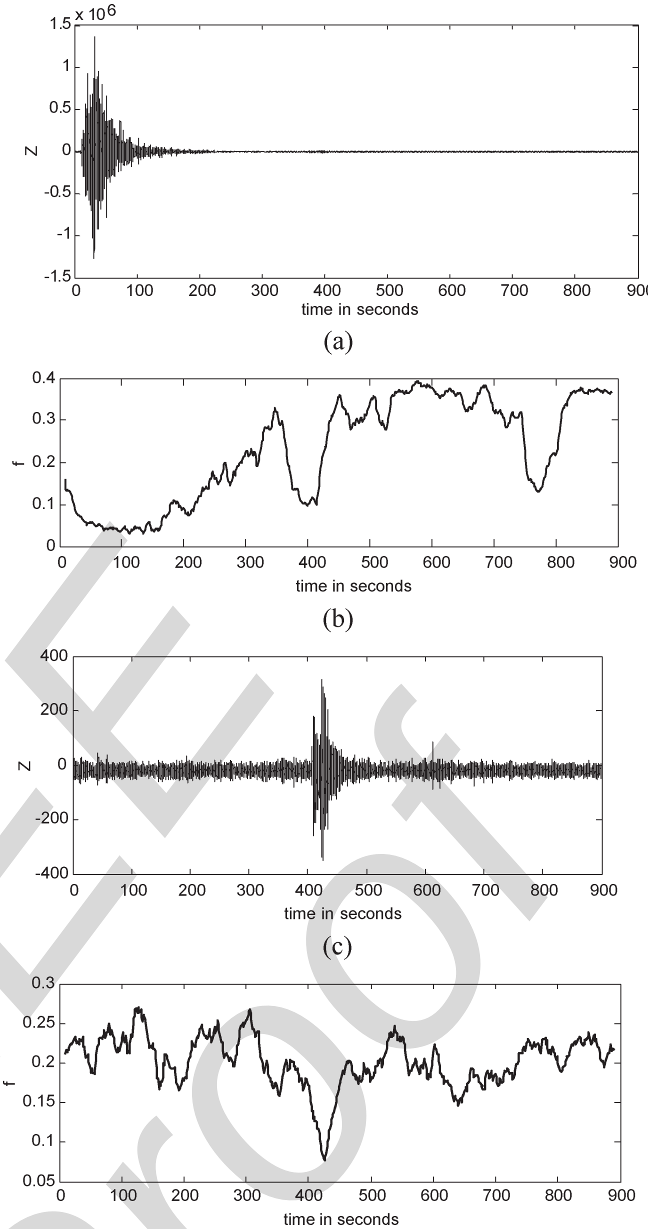

Fig. 3. (a) Vertical component seismogram (z) for the January 8, 2006 earthquake. (b) Frequency of the LM set estimated in 10-s windows for the January 8, 2006 earthquake. (c) Given seismogram for an aftershock. (d) Frequency of the LM set estimated in 10-s windows for the aftershock.

III. P-Phase Picking Based on LMD

The P-phase picking is based on LMD picking. The proposed algorithm consists of several main modules (Fig. 4). As an input, the z component of the seismogram (z signal) for a time period (e.g., 15 min) is used. The proposed method is an extension of [14] and [15], where the signal energy is used in order to detect the P arrival time. The goal of the method is to estimate the most possible time as P-phase arrival of the given seismogram. At the same time, it provides a reliability factor of the estimation. In the case that there is no seismic event at the given seismogram, the reliability factor will be low, denoting "no seismic event."

Initially, the LM sets are estimated in sequential sliding windows. As our experiments show (see Fig. 5), the window length (from 2 to 20 s) does not affect the accuracy of the P estimation. Finally, we have chosen to use 10-s windows.

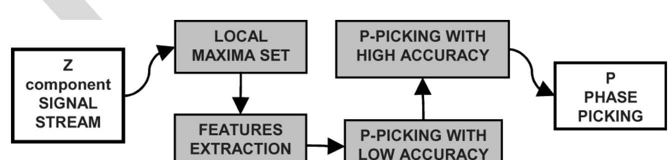

Fig. 4. Scheme of the proposed system architecture.

Then, the proposed features (energy and frequency of LM set) are extracted. The P-phase picking is estimated, using a hierarchical scheme of two stages, in order to minimize the computational cost, similar to the two stages hierarchical estimation of sound signal segmentation proposed in [16]. First, P-picking algorithm is executed yielding the P arrival time with low time accuracy, and then, the P phase is detected within the highest accuracy (the recorded earthquake sampling rate).

More specifically, in the first stage, the mean energies $e_1 = e(LM(W_1)), e_2 = e(LM(W_2))$, the corresponding energy variances σ_1^2, σ_2^2, and the frequencies $f_1 = f(LM(W_1))$, $f_2 = f(LM(W_2))$ of the LM sets of two sequential signal windows W_1 and W_2 locating at time t are estimated, respectively (see Fig. 6).

The windows slide with a shifting rate of 1 s (125 samples). Their symmetric Mahalanobis distance [17], presented by (5),

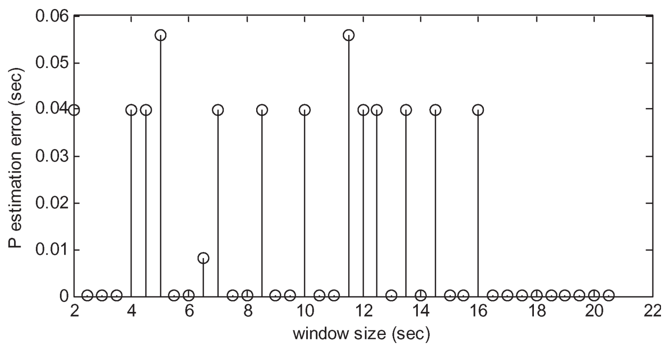

Fig. 5. P estimation error under different window lengths using the seismogram of Fig. 3(c).

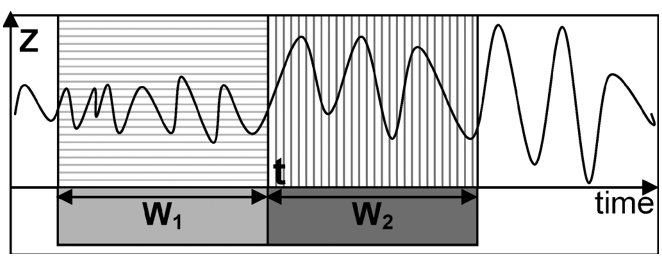

Fig. 6. Two sequential sliding windows W_1 (light-gray horizontal lines) and W_2 (heavy-gray vertical lines) locating at time t on the given seismogram Z.

is used to measure the distance between the two windows over the time t.

$$d(t) = (\mu_1 - \mu_2)^{\mathrm{T}} \cdot \left(\Sigma_1^{-1} + \Sigma_2^{-1}\right) \cdot (\mu_1 - \mu_2) \qquad (5)$$

where μ_1 and μ_2 are the mean feature vectors of signal windows W_1 and W_2. Σ_1 and Σ_2 are the corresponding covariance matrices. Under the assumption that energy and frequency features are uncorrelated, the symmetric Mahalanobis distance can be simplified to

$$\begin{aligned} d(t) &= d_e(t) + d_f(t) \\ d_e(t) &= (e_1 - e_2)^2 \cdot \left(\frac{1}{2 \cdot \sigma_1^2} + \frac{1}{2 \cdot \sigma_2^2}\right) \\ d_f(t) &= \frac{(f_1 - f_2)^2}{2 \cdot \sigma_f^2} \end{aligned} \qquad (6)$$

where σ_f^2 denotes the variance of frequency of the LM set of the whole given signal (e.g., 15 min given signal). This value can be initially estimated before the whole process. The symmetric Mahalanobis distance has been selected, since it outperforms the other frequently used ones like the symmetric Kullback–Leibler (KL2) or Bhattacharyya [18] distance.

$$\mathrm{KL2}(t) = d(t) + 1/2 \cdot tr\left(\Sigma_1\Sigma_2^{-1} + \Sigma_2\Sigma_1^{-1} - 2I\right). \qquad (7)$$

This is due to the fact that the symmetric KL2 contains an extra factor $(tr(\Sigma_1\Sigma_2^{-1} + \Sigma_2\Sigma_1^{-1} - 2I))$, which is maximized when the difference between the variances is maximized, namely, when the time t is located before the real P-phase arrival (the second window has noisy and earthquake samples). Therefore, a false (early) P-phase arrival estimation can be caused. The same problem has been observed under Bhattacharyya distance.

The global maximum (P') of $d(t)$ is taken, and the second stage of the algorithm is initiated. P' corresponds to a first "gross" estimation of P phase with a time accuracy of 1 s due to the window's shifting rate of 1 s from the first stage. Therefore, during the second stage, the two sequential signal windows W_1 and W_2 slide in the region (2-s signal length) close to P' with a shifting rate of one sample, in order to estimate the location of P-phase arrival with the highest accuracy. P corresponds to the position where $d(t)$ is maximized.

$$P = \arg\max\left(d(t)\right). \qquad (8)$$

At this time, the dissimilarity between the two sequential signal windows W_1 and W_2 is maximized, which means that W_1 will correspond to the end of noise, and W_2 will correspond to the rise of the earthquake. Thus, P will be estimated to be the onset of the earthquake. Probably, $d(t)$ will show a local maximum on S phase or other phases arrivals. However, as our experiments show, the global maximum of $d(t)$ is given on P arrival.

The reliability factor of the estimation is obtained from $d(P)$. This value is independent of the signal magnitude [see (5)]. If the given signal does not contain any seismic event (it is just noise), then P-picking module gives very low reliability factor. According to our experiments (using a threshold of 35 on the reliability factor of the estimation), it is observed that 86 out of 88 noisy recordings (15-min duration) were well classified as noise, while the probability of nonrecognition of a seismic event was about 5% using our data set of real seismic events (see Section IV-A).

IV. Experimental Results

In this section, the experimental results of the proposed algorithm, together with comparisons to other algorithms, are presented.

A. Description of Experimental Setup

In order to evaluate the proposed algorithm, a database containing 86 earthquake recordings from six stations (Chania, Rethymno, Heraklion, Sfakia, Ierapetra, and Sitia) was created (see Fig. 7) with a sampling rate of 0.008 Hz. The earthquakes, occurred in the time period between January 8, 2006 and end of June 2006 in the wide area around Crete Island, were first detected by using conventional software (PQL seismic-trace-viewer application). Thereafter, selected earthquake recordings were classified according to their noise content in the following categories: 10 high-"quality" (homogenous and relatively compressed noise—clear view of the seismic event), 40 medium-"quality" (nonhomogenous noise but still clear view of the seismic event), and 36 low-"quality" seismograms (very noisy data, the maximum amplitude of the noise is comparable to the seismic-event maximum amplitude) (see Fig. 8). This classification is implemented by measuring the variance of the noise energy of the LM, normalized to the square of the mean energy (of the noise signal) in order to be independent of the amplitude, using short-time windows (e.g., 1 s).

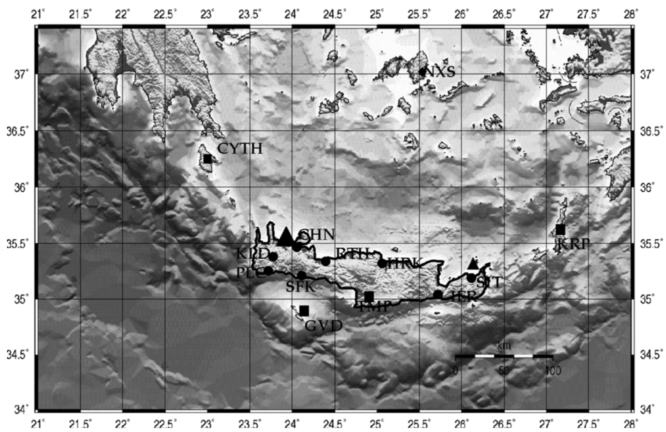

Fig. 7. Topology of the seismological network used in the article covering southern Greece.

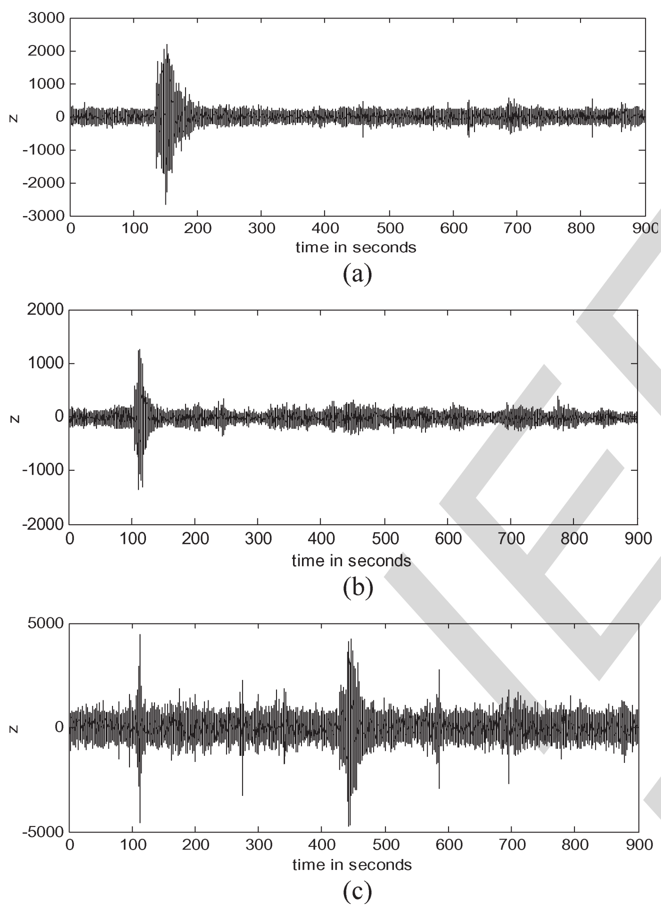

Fig. 8. Examples of (a) high-, (b) medium-, and (c) low-quality seismograms of the used database.

The method has been implemented using MATLAB. We have used a module-based implementation, as shown in Fig. 4. For our experiments, we used a Pentium 4 CPU at 2.8 GHz. A typical processing time for the execution of the proposed scheme is about 25 s for the analysis of a 1-h signal.

B. Results of the Proposed Scheme

Figs. 9 and 10 show results of the proposed algorithm under medium- [Fig. 9(a)] and low- [Fig. 10(a)] "quality" seismograms, respectively. In both figures, the P phase was successfully detected with very high accuracy. Figs. 9(b) and 10(b) show the used symmetric Mahalanobis distance $d(t)$ and its components $d_e(t)$, $d_f(t)$. It holds that, under medium-"quality" seismograms, $d_e(t)$ and $d_f(t)$ [Fig. 9(b)] have about the same graph, showing their global maxima at the same position (estimation of P-phase arrival). On the other hand, in the low-"quality" seismogram [Fig. 10(a)], $d_e(t)$ shows many LM, and its global maximum is not "clear," while $d_f(t)$ appears as "clear" global maximum which corresponds to a local maximum of $d_e(t)$ [Fig. 10(b)]. This location corresponds to the global maximum of $d(t)$ and to the proposed estimation of P-phase arrival. Therefore, this is an example showing that the combination of energy and frequency features is necessary in

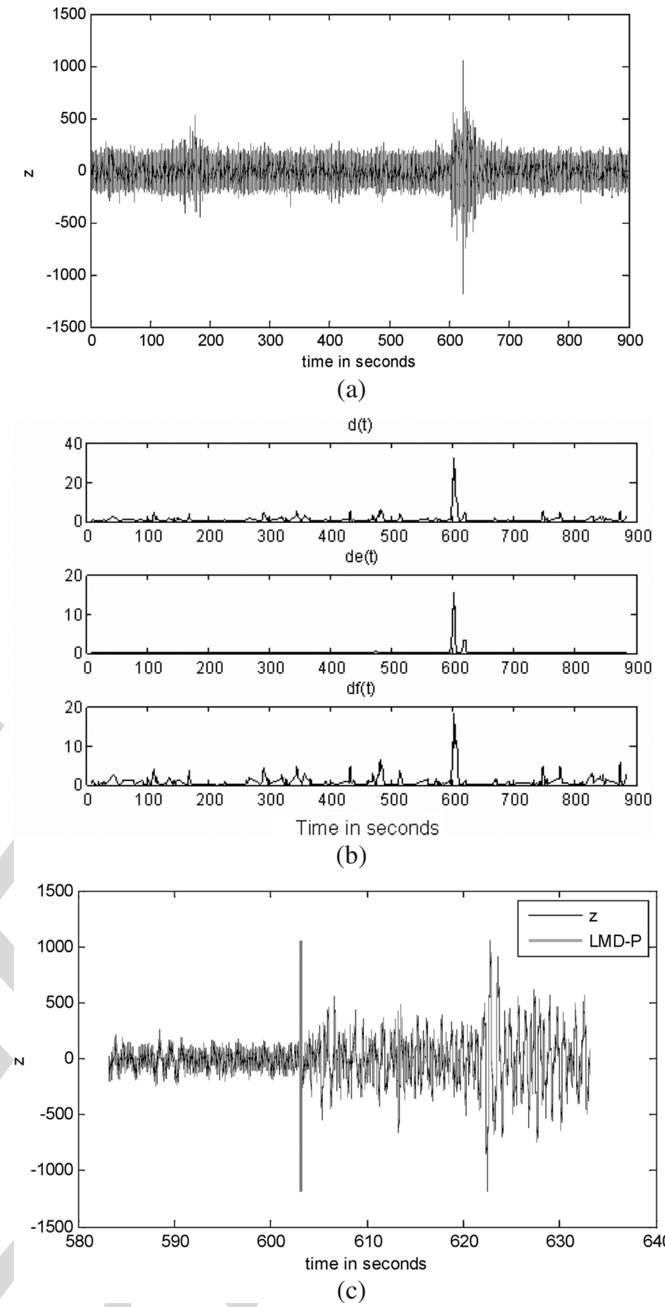

Fig. 9. (a) Medium-"quality" seismogram. (b) $d(t)$, $d_e(t)$, and $d_f(t)$. (c) P-phase picking using the proposed algorithm.

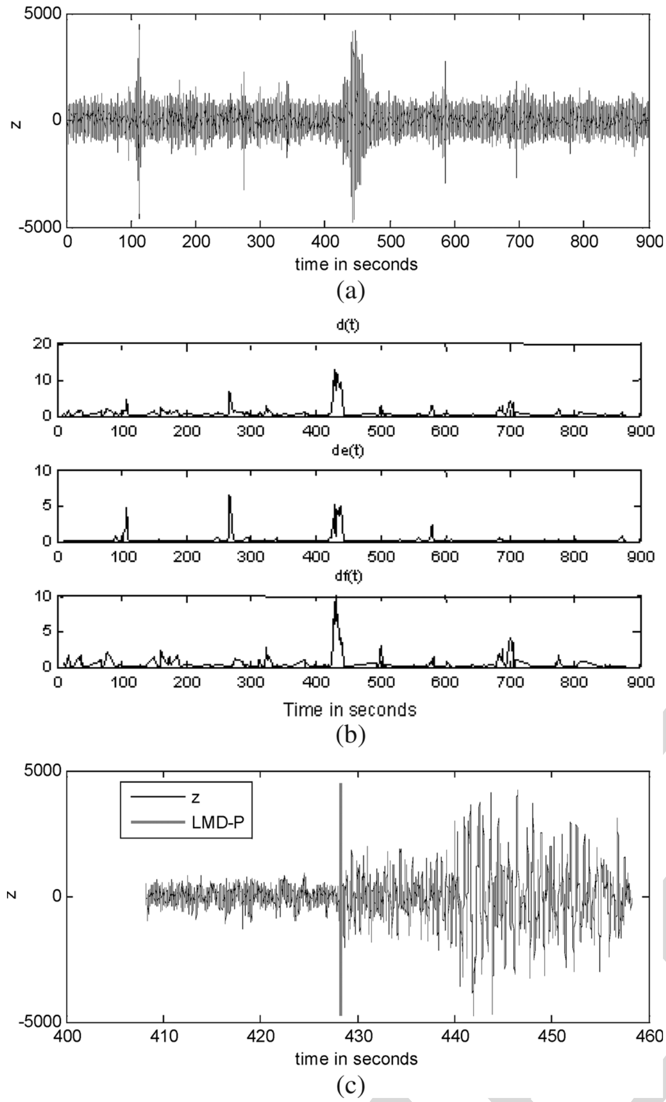

Fig. 10. (a) Low-“quality” seismogram. (b) $d(t)$, $d_e(t)$, and $d_f(t)$. (c) P-phase picking using the proposed algorithm.

order to obtain accurate picking. Figs. 9(c) and 10(c) show the implementation of the presented algorithm on the vertical-component (z) component of the given seismogram in order to specify the earthquake onset.

In order to evaluate the P picking, a database of 86 earthquake recordings was created. The percentage of P picking, which differs to manual picking within a given threshold (e.g., 0.1 s [19]), is about 95%. The wrong P detection was due to very noisy seismograms. We decided to use some very noisy data in order to find out the limitations of the method. Additionally, even in cases of false P detections, it was observed that the picks belonged to the part of the earthquake signal.

C. Comparisons With Other Algorithms

The proposed scheme (LMD-P) has been compared to the P-arrival identification (PAI-S/K) [1] and to the P-arrival-picking-based energy changes (E-P) [14], [15]. The E-P algorithm uses two sequential sliding windows, estimating, as P phase, the time where the ratio between the signal energy of the windows is maximized. It holds that when the second window starts on P arrival, then the first window will end of P arrival. At this time, the ratio of their energy is maximized, since the energy of the seismic event is higher than the energy of noise.

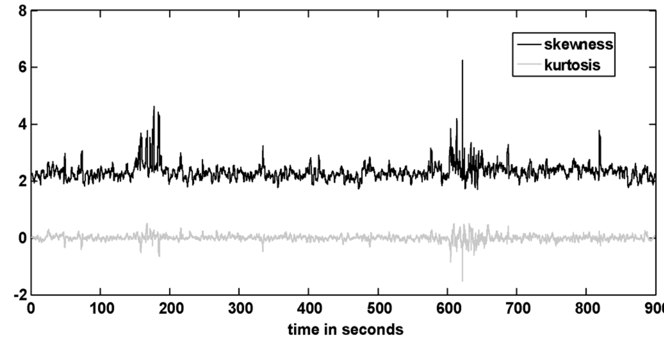

Fig. 11. Results of PAI-S and PAI-K methods on the given seismogram of Fig. 9.

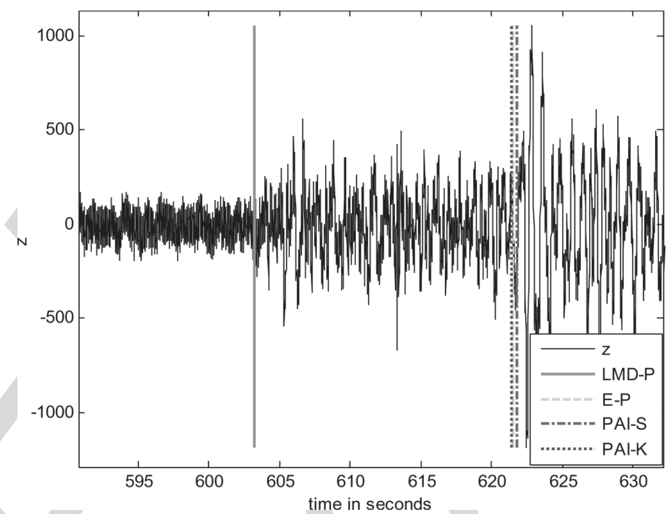

Fig. 12. Results f LMD-P, E-P, PAI-S, and PAI-K methods for P-phase picking projected on the given seismogram of Fig. 9.

The PAI-S/K scheme, consisting of the PAI-S and PAI-K algorithms, uses one sliding window measuring the skewness or kurtosis. When the sliding window contains the recorded noise, as well as the beginning of the seismic event, i.e., the P arrival, the non-Gaussianity and the asymmetry of the corresponding distribution strongly increase, as well as the corresponding skewness and kurtosis of the window. After the P arrival, the distribution of the windowed seismic trace gradually tends to a non-Gaussian although symmetrical one, resulting in an estimated skewness vector that tends almost to zero values. The maximum value (of skewness or kurtosis) is reached only when a sufficient fraction of the time window contains the seismic signal, which is beyond the P-phase arrival. Thus, P arrival is detected by the location of the maximum slope. Fig. 11 shows skewness and kurtosis (results of PAI-S/K algorithm) for the event of Fig. 9. Figs. 12–14 show results of the examined methods.

The comparisons of the proposed algorithm (LMD-P) and other methods (E-P and PAI-S/K) under the whole data set (high-, medium-, and low-“quality” seismograms) are depicted in Table I. The PAI-S/K algorithms outperform Allen’s

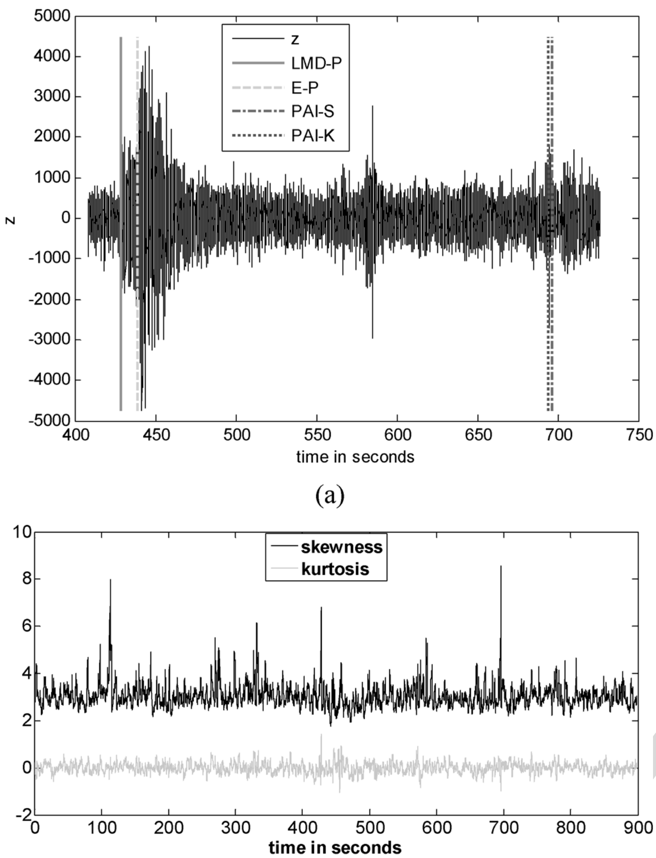

Fig. 13. (a) Results of LMD-P, E-P, PAI-S, and PAI-K methods for P-phase picking projected on the given seismogram of Fig. 10(b) The skewness and kurtosis of the seismograms estimated in 1-s windows.

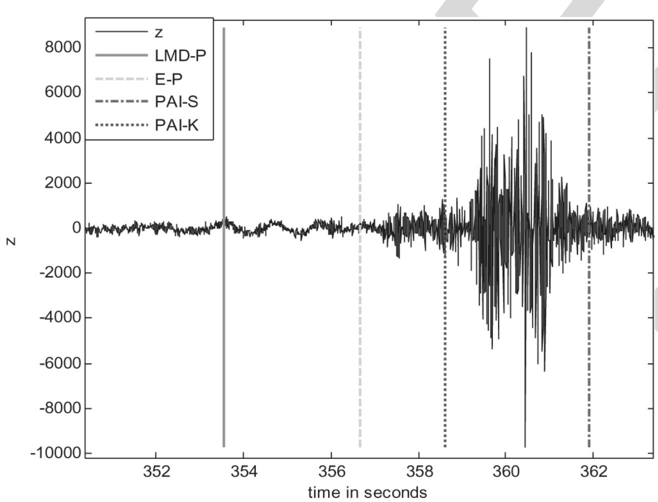

Fig. 14. Results of LMD-P, E-P, PAI-S, and PAI-K methods for P-phase picking projected on the given seismogram.

algorithm [4] in 75% of the cases, while the opposite happens in 6.8% of the cases. Only 18.2% of the cases result to an equal performance. The proposed method outperforms with 95% P-phase detection probability, while E-P, PAI-K, and PAI-S have 88%, 57%, and 60.5%, respectively.

The energy-based feature used by E-P method suffices to detect P phase with time accuracy in high- and medium-"quality"

TABLE I
COMPARISONS OF THE PROPOSED ALGORITHM (LMD-P) AND OTHER METHODS UNDER THE WHOLE DATA SET

Dataset: Method	High Quality	Medium Quality	Low Quality	Total
LMD-P	100% (10/10)	95% (38/40)	94.44% (34/36)	95.35% (82/86)
E-P	100% (10/10)	92.5% (37/40)	80.56% (29/36)	88.37% (76/86)
PAI-K	70% (7/10)	60% (24/40)	50% (18/36)	56.98% (49/86)
PAI-S	70% (7/10)	65% (26/40)	52.78% (19/36)	60.47% (52/86)

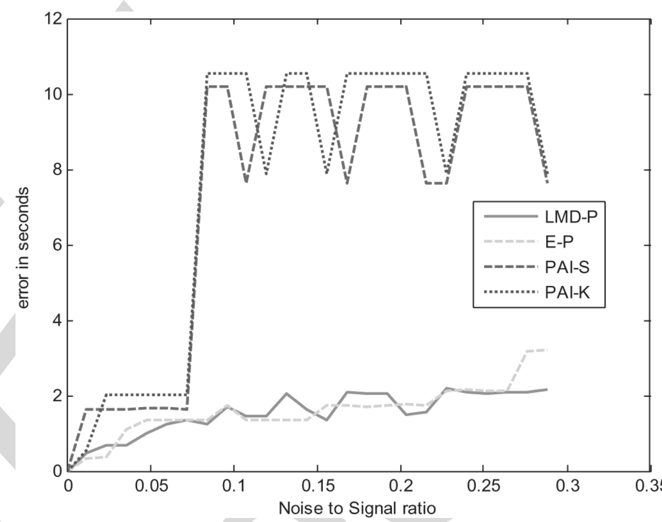

Fig. 15. P-detection errors (in seconds) in respect to noise-to-signal ratio for the seismogram of Fig. 3 under LMD-P, E-P, PAI-S, and PAI-K methods.

seismograms. However, in low-"quality" seismograms, the energy of noise and seismic event is similar; thus, the detection probability decreases. In these cases, the E-P algorithm cannot identify the seismic event, since the envelope of the seismic trace does not change sufficiently. Concerning the PAI-S/K method, it gives accurate in-time results, but there is a probability of false detection. This is due to the fact that the used skewness and kurtosis [see Figs. 11 and 13(b)] are sensitive to noise effects. The proposed method combines robust energy- and frequency-based features yielding the best performance under any type of given seismograms (see Figs. 12, 13(a), and 14). Moreover, the robustness of the proposed method and the comparison with the rest of the algorithms is examined by the experiment of Fig. 15. It shows the P detection error (in seconds) with respect to noise-to-signal ratio for the January 8, 2006 earthquake z signal. Gaussian white noise was added in order to implement this experiment. It is observed that the error of the proposed method increases smoothly with respect to the noise energy. The error in the detection of P arrival (LMD-P and E-P methods) is reaching a maximum value of 2 s by increasing the noise-to-signal ratio. On the other hand, PAI-S/K method is getting a P detection error of about 10 s for noise-to-signal ratio greater than 0.5.

V. Conclusion

The main contribution of this paper concerns the proposed seismogram analysis using robust and simple energy–frequency-based features that suffice for an earthquake detection and high time accuracy of P-arrival estimation. The combination of energy- and frequency-based features suffices for high time-accuracy P-phase arrival picking under any type of seismic data. The implementation of the proposed algorithm is based on LMD of a given seismogram. The detection of P arrival is controlled by a reliability factor. Moreover, this factor can be used for automatic rejection of noise signals. The comparison with two alternative techniques given in literature suggests the great performance and the robustness of the proposed scheme in a sufficient seismogram database.

As future work, we plan to extend the proposed method on S-arrival estimation and on P-converted-phases estimation between the P and S first arrivals.

Acknowledgment

The authors would like to thank the anonymous reviewers for the critical review and constructive comments.

References

[1] C. D. Saragiotis, L. J. Hadjileontiadis, and S. M. Panas, "PAI-S/K: A robust automatic seismic P phase arrival identification scheme," *IEEE Trans. Geosci. Remote Sens.*, vol. 40, no. 6, pp. 1395–1404, Jun. 2002.

[2] O. H. Colak, "P phase and S phase detection using the daubechies wavelet transform (dWT) to minimize the noise at three component seismograms displacement records," in *Proc. Eur. Signal Process. Conf.*, Antalya, Turkey, 2005.

[3] "Advances in seismic event location," in *Modern Approaches in Geophysics*, C. Thurber and N. Rabinowitz, Eds. Dordrecht, The Netherlands: Kluwer, 2000.

[4] R. Allen, "Automatic earthquake recognition and timing from simple traces," *Bull. Seismol. Soc. Amer.*, vol. 68, no. 5, pp. 1521–1532, Oct. 1978.

[5] K. R. Gledhill, "An earthquake detector employing frequency domain techniques," *Bull. Seismol. Soc. Amer.*, vol. 75, no. 6, pp. 1827–1835, Dec. 1985.

[6] P. Goldstein, D. Dodge, and M. Firpo, *SAC2000: Signal processing and analysis tools for seismologists and engineers*, 1999. UCRL-JC-135963, Invited contribution to the IASPEI International Handbook of Earthquake and Engineering Seismology.

[7] C. A. Rowe, R. C. Aster, B. Borchers, and C. J. Young, "An automatic, adaptive algorithm for refining phase picks in large seismic datasets," *Bull. Seismol. Soc. Amer.*, vol. 92, no. 5, pp. 1660–1674, Jun. 2002.

[8] H. Zhang, C. Thurber, and C. Rowe, "Automatic P-wave arrival detection and picking with multiscale wavelet analysis for single-component recordings," *Bull. Seismol. Soc. Amer.*, vol. 93, no. 5, pp. 1904–1912, Oct. 2003.

[9] B. O. Ruud, C. D. Lindholm, and E. S. Husebye, "An exercise in automating seismic record analysis and network bulletin production," *Bull. Seismol. Soc. Amer.*, vol. 83, no. 3, pp. 660–679, Jun. 1993.

[10] K. S. Anant and F. U. Dowla, "Wavelet transform methods for phase identification in three-component seismograms," *Bull. Seismol. Soc. Amer.*, vol. 87, no. 6, pp. 1598–1612, Dec. 1997.

[11] C. Panagiotakis, I. Grinias, and G. Tziritas, "Automatic human motion analysis and action recognition in athletics videos," in *Eur. Signal Process. Conf.*, 2006.

AQ2

[12] P. R. Krishnaiah and P. K. Sen, Eds., *Handbook of Statistics: Nonparametric Methods*. Amsterdam, The Netherlands: North-Holland, 1984.

[13] Y. Rubner, C. Tomasi, and L. J. Guibas, "A metric for distributions with applications to image databases," in *Proc. IEEE Int. Conf. Comput. Vis.*, Jan. 1998, pp. 59–66.

[14] E. Kokinou, C. Panagiotakis, and F. Vallianatos, "Earthquake/noise discrimination and estimation of P–S phases based on wave characteristics," in *Proc. 11th Int. Congr. Bull. Geol. Soc. Greece*, 2007, pp. 1138–1149.

[15] E. Kokinou, C. Panagiotakis, and F. Vallianatos, "Seismic phase picking based on wave characteristics," in *Proc. EGU Gen. Assem.*, Vienna, Austria, 2007. EGU2007-A-08898.

[16] C. Panagiotakis and G. Tziritas, "A speech/music discriminator based on RMS and zero-crossings," *IEEE Trans. Multimedia*, vol. 7, no. 1, pp. 143–154, Feb. 2005.

[17] S. Kevin Zhou and R. Chellappa, "From sample similarity to ensemble similarity: Probabilistic distance measures in reproducing kernel Hilbert space," *IEEE Trans. Pattern Anal. Mach. Intell.*, vol. 28, no. 6, pp. 917–929, Jun. 2006.

[18] P. Mahalanobis, "On the generalized distance in statistics," in *Proc. Nat. Inst. Sci. India*, 1936, vol. 12, pp. 49–55.

[19] J. Wang and T.-L. Teng, "Identification and picking of S phase using an artificial neural network," *Bull. Seismol. Soc. Amer.*, vol. 87, no. 5, pp. 1140–1149, Oct. 1997.

Costas Panagiotakis received the B.A., M.Sc., and Ph.D. degrees in computer science from the Computer Science Department, University of Crete, Heraklion, Greece, in 2001, 2003, and 2007, respectively.

He is currently with the Department of Computer Science, University of Crete. His interests include video-image analysis, pattern recognition, signal processing, computer graphics, and algorithms.

Eleni Kokinou received the B.A. degree from the Geology Department, Aristotelian University of Thessaloniki, Thessaloniki, Greece, in 1993 and the M.Sc. and Ph.D. degrees in geophysics from the Technical University of Crete, Chania, Greece, in 1998 and 2002, respectively.

She is currently an Assistant Professor with the Laboratory of Geophysics and Seismology, Department of Natural Resources and Environment, Technological Educational Institute of Crete, Heraklion, Greece. Her interests include geophysics, particularly reflection and refraction seismology, signal processing, and algorithms.

Filippos Vallianatos received the B.A. and Ph.D. degrees in physics from the Physics Department, University of Athens, Athens, Greece, in 1985 and 1989, respectively.

He is a Professor with the Laboratory of Geophysics and Seismology, Department of Natural Resources and Environment, Technological Educational Institute of Crete, Heraklion, Greece. His interests include geophysics, physics of the earth's interior, and natural hazards.

AUTHOR QUERIES

AUTHOR PLEASE ANSWER ALL QUERIES

AQ1 = Please validate the address provided for the Technological Educational Institute of Crete.
AQ2 = Please provide page range on Ref. [11].

ATTN: If you are paying to have all or some of your figures appear in color in the print issue, it is very important that you fill out and submit a copy of the IEEE Page Charge & Reprint Form along with your proof corrections. This form is available from the same URL where these page proofs were downloaded from. Thank you.

END OF ALL QUERIES